A&A 484, 267–273 (2008)
DOI: 10.1051/0004-6361:200809346

Astronomy & Astrophysics

High-energy neutrino emission from shell-type supernova remnants

J. Fang[1], L. Zhang[1], C. Y. Yang[1], G. F. Lin[1], and A. M. Zheng[2]

[1] Department of Physics, Yunnan University, Kunming, PR China
e-mail: fangjun1653@126.com
[2] Department of Physics, Zhaotong College, Zhaotong, PR China

Received 2 January 2008 / Accepted 26 March 2008

ABSTRACT

Based on a time-dependent model of particle production and non-thermal photon emission, we study high-energy neutrino emission from shell-type supernova remnants (SNRs). In such a model, particles are accelerated to relativistic energies through the shock acceleration mechanism and evolve with time in an SNR. For a given SNR, therefore, the temporal evolution of the particle energy distribution, the non-thermal spectrum of photons, and the spectrum of neutrinos can be calculated numerically. We apply the model to two young SNRs, G347.3−0.5 and G266.2−1.2, and two old ones, G8.7−0.1 and G23.3−0.3. For each SNR, we determine the parameters involved in the model by comparing the predicted non-thermal spectrum with the observed radio, X-ray and γ-ray data. We study the properties of the corresponding neutrino emission, including the neutrino spectrum and the event rates expected in the next-generation km^3-scale neutrino telescope, KM3NeT. Our results indicate that the high-energy TeV γ-rays from the four SNRs are produced predominately via hadronic interaction and that young SNRs such as G266.2−1.2 and G347.3−0.5 are the potential neutrino sources whose neutrinos are most likely to be identified by next-generation km^3 neutrino telescopes.

Key words. gamma rays: theory – neutrinos – radiation mechanisms: non-thermal – supernova remnants

1. Introduction

SNRs are of prime candidates for acceleration of Galactic cosmic rays by the diffusive shock wave acceleration process (Reynolds 1996; Hillas 2005; Ellison et al. 2007). In recent years, very high-energy (VHE) γ-rays have been detected from some SNRs and those VHE photons can be interpreted as either soft photons up-scattered by relativistic electrons (Katagiri et al. 2005) or hadronic γ-rays from proton-proton (p-p) interactions as high-energy protons collide with the ambient matter in an SNR (Enomoto et al. 2002; Pannuti et al. 2003; Lazendic et al. 2004). Obviously, if the VHE γ-rays from an SNR are of hadronic origin, the high-energy neutrino emission may be significant and the neutrino signal probably could be detected by current neutrino telescopes, such as AMANDA and IceCube (Bednarek et al. 2005), and by the next-generation neutrino telescope, KM3NeT, with an instrument volume of 1 km^3 (Kappes et al. 2007).

Hadronic interpretations of TeV γ-rays from SNRs have been widely proposed. The young SNR G347.3−0.5 has been detected twice by HESS and is the most intense shell-type SNR in the TeV γ-ray sky (Vissani 2006). The CANGAROO collaboration has indicated that the spectrum of the VHE γ-rays from the SNR matches that expected if the γ-rays are produced via π^0 decay from proton-proton collisions (Enomoto et al. 2002). Therefore, the SNR G347.3−0.5 is an important potential neutrino source which can be identified as a discrete neutrino source by neutrino telescopes. More recently, a survey of the inner part of the Galactic Plane in VHE γ-rays has been performed with the HESS Cherenkov telescope system. Aharonian et al. (2006b) presented detailed spectral and morphological information of some new sources along with discussion of possible counterparts in other wavelength bands. Some TeV sources discovered in the survey, such as HESS J1804−216 and HESS J1834−087, can be associated with old SNRs (Aharonian et al. 2006b; Fang & Zhang 2008; Tian et al. 2007), and the TeV photons from the old SNRs are probably of hadronic origin because high-energy protons can exist for a long time due to the long energy loss time for p-p interactions (Fang & Zhang 2008). Thus, old TeV SNRs are also important possible neutrino sources in the Galaxy.

The neutrino spectrum for a given SNR with observed TeV photons can be estimated by assuming that the TeV γ-rays are produced predominately via hadronic processes (Carr et al. 2007; Kappes et al. 2007; Kistler& Beacom 2006). In this paper, we use the time-dependent model in Fang & Zhang (2008) with which the evolved non-thermal spectra of both the primary particles accelerated directly by the shock wave and the secondaries produced via p-p interaction can be calculated numerically. We investigate the high-energy neutrino emission from shell-type SNRs and estimate the detected neutrino signals that may be measured by the next-generation telescope, KM3NeT, using the newest simulation results in Carr et al. (2007). The parameters involved in the model for a given source can be limited by comparison of the calculation results with the multi-wavelength observations, and then the corresponding neutrino spectra can be calculated. This paper is organized as follows. The calculation model are briefly illustrated in Sect. 2. The results from the applications of the model to two young SNRs, G347.3−0.5 and G266.2−1.2, and two old ones, G8.7−0.1 and G23.3−0.3, are shown in Sect. 3. The main conclusions and some discussion are given in Sect. 4.

2. Temporal-evolving model for particle and photon spectra

Originally, Sturner et al. (1997) presented a temporal-evolving model for non-thermal particle and photon spectra at different

stages in the lifetime of a shell-type SNR. Zhang & Fang (2007) modified the model to explain the multi-waveband observations of young SNRs and shown that the TeV γ-rays from the two young shell-type SNRs, G347.3−0.5 and G266.2−1.2, are primarily of hadronic origin. Moreover, Fang & Zhang (2008) studied the non-thermal emission from old SNRs by including the evolution of secondary electrons and positrons produced in p-p interactions in the model, and applied the model to two old SNRs, G8.7−0.1 and G23.3−0.3. Their results indicated that the VHE γ-rays with energies above 1 TeV from the two SNRs mainly had hadronic origin. In this section, we first review the model for non-thermal particle and photon spectra, and then give the detailed formula that we use to tackle the p-p interactions in which high-energy photons and neutrinos are produced.

2.1. Temporal evolution of particle energy distribution

The analytical model of shock dynamics of SNRs expanding into the uniform ambient medium with a constant density $n_{\rm ISM}$ and a magnetic field strength $B_{\rm ISM}$ is used to describe the SNR evolution (see details in Sturner et al. 1997). The density and the magnetic field strength of the upstream and downstream regions of the shock satisfy the following relations: $n_{\rm down} = rn_{\rm up}$ and $B_{\rm down} = rB_{\rm up}$, where the shock compression ratio $r \sim 4$ for a strong shock, neglecting nonlinear effects (Sturner et al. 1997). In the analytical model, assuming the initial explosion energy of an SNR is $E = 10^{51}E_{51}$ ergs, and the initial velocity of the shock is v_0, the SNR evolves through three stages : the free expansion stage (shock velocity $v_{\rm s}(t) = v_0$ for $t \le t_{\rm Sed} = (3E/2\pi m_{\rm H}n_0v_0^5)^{1/3} \approx 2.1\times10^2(E_{51}/n_0)^{1/3}v_0^{-5/3}$ yr), the Sedov stage ($v_{\rm s}(t) \propto t^{-3/5}$ for $t_{\rm Sed} < t \le t_{\rm Rad} \approx 4.0\times10^4E_{51}^{4/17}n_0^{-9/17}$ yr), and the radiative stage ($v_{\rm s}(t) \propto t^{-2/3}$ for $t > t_{\rm Rad}$), where $n_0 = \mu n_{\rm ISM}$, $\mu = 1.4$ is the mean atomic weight of the interstellar medium assuming 1 helium atom for every 10 hydrogen atoms, and $m_{\rm H}$ is the mass of hydrogen; for simplicity, the hydrogen inside the SNR is assumed to be fully ionized and the SNR interior is thought to be homogenous. This does not affect the final result because the resulting non-thermal spectrum only relates to the initial spectrum and the total number of the instantaneously accelerated particles, and the subsequent evolution, with a constant density $n_{\rm SNR} = 4n_{\rm ISM}$ and a magnetic field strength $B_{\rm SNR} = 4B_{\rm ISM}$. The non-thermal charged particles inside the SNR are produced through diffusive shock acceleration, after taking the particle's energy-loss processes and the effect of the free escape from the shock region into account. The volume-averaged emissivity, $Q(E,t) = {\rm d}N/{\rm d}V{\rm d}t{\rm d}E$, of the shock accelerating electrons and protons are approximated as

$$Q_{\rm e}(E,t) = Q_{\rm e}^0G(t)[E(E+2m_{\rm e}c^2)]^{-[(\alpha+1)/2]}(E+m_{\rm e}c^2) \times\exp\left(-\frac{E}{E_{\rm e,max}(t)}\right), \quad (1)$$

and

$$Q_{\rm p}(E,t) = Q_{\rm p}^0G(t)[E(E+2m_{\rm p}c^2)]^{-[(\alpha+1)/2]}(E+m_{\rm p}c^2) \times\exp\left(-\frac{E}{E_{\rm p,max}(t)}\right), \quad (2)$$

where E is the particle kinetic energy, and m_e and m_p are the electron mass and proton mass, $\alpha \ge 2.0$ is the spectral index (Sturner et al. 1997). For particles accelerated in the shock of an SNR, the power law particle spectra do not extend to infinite energy and must be truncated by three mechanisms, namely, the finite age of the SNR, the energy-loss processes, and the free escape from the shock region (Sturner et al. 1997; Zhang & Fang 2007). The maximum kinetic energy of electrons and protons, $E_{e,\,\rm max}$ and $E_{p,\,\rm max}$, can be calculated with Eqs. (3)–(5) in Zhang & Fang (2007), where a parameter is the maximum wavelength of MHD turbulence $\lambda_{\rm max}$, which is set to 2×10^{17} cm as in Fang & Zhang (2008). Physically, MHD turbulence results in repeated scattering of a charged particle across the shock front, which is $f \sim 1$ times the particle gyroradius ($r_{\rm L} = E/Be$) and the free-escape energy is given by $eB_{\rm ISM}\lambda_{\rm max}/f$ (Struner et al. 1997). The particles with energies above the free-escape energy will escape the shock quickly. The function $G(t)$ is given by

$$G(t) = \begin{cases} [R_{\rm SNR}(t_{\rm Sed})/R_{\rm SNR}(t)] & t \le t_{\rm rad} \\ 0 & t > t_{\rm rad}, \end{cases} \quad (3)$$

where $R_{\rm SNR}(t) = \int v_{\rm s}(t){\rm d}t$, which means that the SNR shock produces a constant number of energetic particles per unit SNR surface area until the SNR enters the radiative phase when the source turns off (Sturner et al. 1997); a part of the energy in the ejecta with initial mass $M_{\rm ej}$ and initial velocity v_0, which is set to 10^9 cm s^{-1} in this paper, is converted into the kinetic energy of both injected electrons and protons, i.e. $E_{\rm par} = \eta M_{\rm ej}v_0^2/2$, where η, which is set to 0.1, is the conversion efficiency. On the other hand, the kinetic energy can be expressed as

$$E_{\rm par} = \int_0^{t_{\rm rad}}{\rm d}tV_{\rm SNR}(t)[\int_0^{E_{\rm e,max}}{\rm d}EEQ_{\rm e}(E,t) + \int_0^{E_{\rm p,max}}{\rm d}EEQ_{\rm p}(E,t)], \quad (4)$$

and $V_{\rm SNR}(t) = 4\pi R_{\rm SNR}^3(t)/3$ is the SNR volume. Therefore, introducing the parameter $K_{\rm ep} = Q_{\rm e}^0/Q_{\rm p}^0$, we can estimate factors $Q_{\rm e}^0$ and $Q_{\rm p}^0$ using Eq. (4).

Once the volume-averaged emissivities of the shock accelerated particles are given for a certain SNR, the temporal evolution of the particle energy distribution can be obtained by solving the Fokker-Planck equations for both electrons and protons in energy space, which are given by

$$\frac{\partial n_{\rm e}(E_{\rm e},t)}{\partial t} = -\frac{\partial}{\partial E_{\rm e}}\left[\dot{E}_{\rm e}^{\rm tot}n_{\rm e}(E_{\rm e},t)\right] + \frac{1}{2}\frac{\partial^2}{\partial E_{\rm e}^2}\left[D(E_{\rm e},t)n_{\rm e}(E_{\rm e},t)\right] + Q_{\rm e}(E_{\rm e},t) - \frac{n_{\rm e}(E_{\rm e},t)}{\tau}, \quad (5)$$

and

$$\frac{\partial n_{\rm p}(E_{\rm p},t)}{\partial t} = -\frac{\partial}{\partial E_{\rm p}}\left[\dot{E}_{\rm p}^{\rm tot}n_{\rm p}(E_{\rm p},t)\right] + \frac{1}{2}\frac{\partial^2}{\partial E_{\rm p}^2}\left[D(E_{\rm p},t)n_{\rm p}(E_{\rm p},t)\right] + Q_{\rm p}(E_{\rm p},t) - \frac{n_{\rm p}(E_{\rm p},t)}{\tau}. \quad (6)$$

$n_{\rm e}(E_{\rm e},t)$ and $n_{\rm p}(E_{\rm e},t)$ represent the differential densities of the accelerated electrons and protons at each moment during the SNR lifetime; the corresponding volume-averaged electron and proton densities are $J_{\rm e}(E_{\rm e},t) = (c\beta/4\pi)n_{\rm e}(E_{\rm e},t)$ and $J_{\rm p}(E_{\rm p},t) = (c\beta/4\pi)n_{\rm p}(E_{\rm p},t)$. c is the light speed and β is the particle speed in units of c. The terms on the right-hand sides in Eqs. (5) and (6) represent systematic energy losses, diffusion in energy space, the particle source function and catastrophic energy loss (see details in Fang & Zhang 2008).

2.2. Photon emission and high-energy neutrino production

For a given SNR, the time-dependent electron and proton intensities can be obtained by solving Eqs. (5) and (6), so the multi-wavelength non-thermal photon spectrum can be calculated. These photons can be produced by electron synchrotron radiation, bremsstrahlung, inverse Compton scattering of the CMB, Galactic IR and optical background, and neutral pion decay gamma-rays from the proton-proton interaction. The details of the photon emission can be seen in Fang & Zhang (2008). Here, we introduce the high-energy neutrino production processes briefly.

The corresponding volume-averaged emissivities for secondary particles, γ, $e^{\pm}$, ν_e, $\bar{\nu}_e$, ν_μ, $\bar{\nu}_\mu$, produced in the p-p interactions can be given by

$$Q^0_{\rm sec}(E_{\rm sec}, t) = 4\pi\mu_{\rm pp} n_{\rm SNR} \int {\rm d}E_{\rm p} J_{\rm p}(E_{\rm p}, t) \frac{{\rm d}\sigma(E_{\rm sec}, E_{\rm p})}{{\rm d}E_{\rm sec}}, \quad (7)$$

where $\mu_{\rm pp} = 1.45$ is an enhancement factor for collisions involving heavy nuclei in an SNR (Sturner et al. 1997). Kamae et al. (2006) presented a series of accurate, convenient parameterized formulae to calculate the spectra of stable secondary particles (γ, $e^{\pm}$, ν_e, $\bar{\nu}_e$, ν_μ, $\bar{\nu}_\mu$) in the p-p interactions, which greatly facilitate calculations involving p-p interaction in astronomical environments. The formulae were derived from the latest p-p interaction model given in Kamae et al. (2005), which incorporates the logarithmically rising inelastic cross section, the diffraction dissociation process, and the Feynman scaling violation. The functional formula reproducing the secondary particle spectra include the nondiffractive, diffractive, and resonance-excitation components ($\Delta(1232)$ and res(1600)). The details of the calculation can be seen in Fang & Zhang (2008) and Kamae et al. (2006).

Three flavor oscillations of neutrinos should be considered to obtain the observed neutrino flux on the Earth for an SNR. After propagation, the neutrino flux can be expressed as

$$F_l = \frac{V_{\rm SNR}}{4\pi d^2} \sum_{l'=e,\mu,\tau} P_{ll'} Q^0_{\nu_{l'}}, \quad (8)$$

where d is the distance from the earth to the SNR, and the matrix P can be approximated as (Costantini & Vissani 2005)

$$P \sim \begin{bmatrix} 0.6 & 0.2 & 0.2 \\ 0.2 & 0.4 & 0.4 \\ 0.2 & 0.4 & 0.4 \end{bmatrix}. \quad (9)$$

Note that Cavasinni et al. (2006) investigated the TeV neutrinos from embedded SNRs, and gave a more detailed computation of the γ-ray to neutrino flux ratio. The matrix P in the paper shows small differences to that in Costantini & Vissani (2005). However, we still use the matrix in Costantini & Vissani (2005) for the calculations.

Many astrophysical TeV γ-ray sources have been detected in recent years, and km^3 scale detectors are needed to investigate the corresponding neutrinos (Carr et al. 2007). The event rate in a neutrino telescope can be calculated by (Kappes et al. 2007)

$$N_\nu = R_{\Theta_{\rm opt}} \int {\rm d}t \int {\rm d}E_\nu A^{\rm eff}_\nu \frac{{\rm d}N_\nu}{{\rm d}E_\nu}, \quad (10)$$

where the integration considers the observation time when the source is below the horizon, $R_{\Theta_{\rm opt}} = 0.72$ is the reduction factor taking into account the neutrino loss outside the search window, $A^{\rm eff}_\nu$, which comprises the neutrino attenuation inside the Earth, the neutrino conversion probability, and the muon detection efficiency, to the neutrino effective area of the detector. ${\rm d}N_\nu/{\rm d}E_\nu$ is the neutrino spectrum on the Earth. Recently, Carr et al. (2007) investigated the sensitivity to points sources of KM3NeT for two different configurations and reported the neutrino effective areas using a full simulation and reconstruction chain. We use the effective areas for configuration 2 (see Fig. 1 in Carr et al. 2007) to estimate the event rates for each SNR in KM3NeT after years of observations.

3. Applications to SNRs

We now apply the time-dependent model of non-thermal particle, photon and neutrino spectra to SNRs. The unknown parameters involved in the model are usually limited by comparison of the model result with the multi-band observations for a given SNR (Zhang & Fang 2007; Fang & Zhang 2008). We fit the parameters empirically due to the many uncertainties in the model such as the age, the distance, the initial ejected mass, the initial velocity of the shock, the conversion efficiency, and in the observations, especially in the X-ray band for an SNR. Firstly, a set of appropriate parameters are chosen to describe the multi-wavelength non-thermal emission for each SNR, and then the corresponding neutrinos from the SNR can be investigated. In this section, the model is applied to two young SNRs, G347.3−0.5 and G266.2−1.2, and two old ones, G8.7−0.1 and G23.3−0.3.

3.1. G347.3−0.5

The shell-type SNR G347.3−0.5 (RX J1713.7−3946), which is compatible with a core collapse supernova that exploded in A.D. 393 at a distance of about 1 kpc (Wang et al. 1997), is a prominent potential neutrino source that probably would be detected by KM3NeT. VHE γ-rays from the SNR have been detected with HESS, and the hard differential γ-ray spectrum, measured over two orders of magnitude from 190 GeV to 40 TeV, deviates from a power law distribution above 10 TeV (Aharonian et al. 2006a). X-ray observations indicate that the non-thermal X-ray spectrum for the whole SNR has a power-law with index of ∼2.4 although the spectra in different regions have slightly different photon indexes (Slane et al. 1999), so we adopt that the non-thermal X-ray spectrum of the whole SNR is a power law with photon index 2.4 and the flux from 0.5–10 keV is $F_{\rm X}$(0.5–10 keV) $= 6.6 \times 10^{-10}$ erg cm^{-2} s^{-1}. The high-resolution radio observations were performed with the Australia Telescope Compact Array (ATCA) (Lazendic et al. 2004). Note that the radio flux given in their paper is just for the northwest part of the shell so we multiply by a factor of two to account for the whole SNR, as treated in Aharonian et al. (2006a).

The probable neutrino signals in KM3NeT for the SNR G347.3−0.5 have been investigated by assuming that the TeV γ-ray photons are predominately of hadronic origin (Kistler & Beacon 2006; Kappes et al. 2007; Carr et al. 2007), and that the expected event rates ($E_\nu > 1$ TeV) is about 10 in 5 yrs of observations. It had been shown that, for a given SNR with specific age and distance, the parameters involved in the model can be limited by comparison of the model results with multi-band observations (Zhang & Fang 2007; Fang & Zhang 2008). For the SNR G347.3−0.5, we use an age of 1600 yr and a distance of 1 kpc, and choose other appropriate parameters to model the multi-band emission. The details of the parameters used are shown in Table 1, and the resulting photon and neutrino spectra are illustrated in Fig. 1. Obviously, the non-thermal emission from radio to hard X-ray bands is predominately from the

Table 1. The parameters used and the expected neutrino event rates in KM3NeT after five years of observation for each SNR. The visibility indicates the fraction of time when the source is below the horizon to KM3NeT, and we take the visibility and the expected atmospheric neutrino event rates for each source from Kappes et al. (2007).

Model parameter	Symbol	G347.3−0.5	G266.2−1.2	G8.7−0.1	G23.3−0.3
Particle spectral index	α	2.0	2.1	2.0	2.0
Initial ejected mass	$M_{\rm ej}$	2.0 $M_\odot$	2.0 $M_\odot$	1.5 $M_\odot$	1.5 $M_\odot$
Age	T	1600 yr	1000 yr	18 000 yr	80 000 yr
Distance	d	1.0 kpc	0.3 kpc	6 kpc	4.2 kpc
Ambient hydrogen density	$n_{\rm ISM}$	12 cm^{-3}	7 cm^{-3}	6 cm^{-3}	10 cm^{-3}
Ambient magnetic field strength	$B_{\rm ISM}$	13 μG	30 μG	6 μG	7 μG
Electron proton ratio	$K_{\rm ep}$	0.012	0.002	0.15	0.2
Visibility	$f_{\rm v}$	0.74	0.83	0.61	0.54
Expected neutrino event rates	N(>1 TeV)	7.6	11.3	0.9	0.5
Expected atmospheric neutrino event rates	$N_{\rm atm}$(>1 TeV)	41	104	8.4	6.0

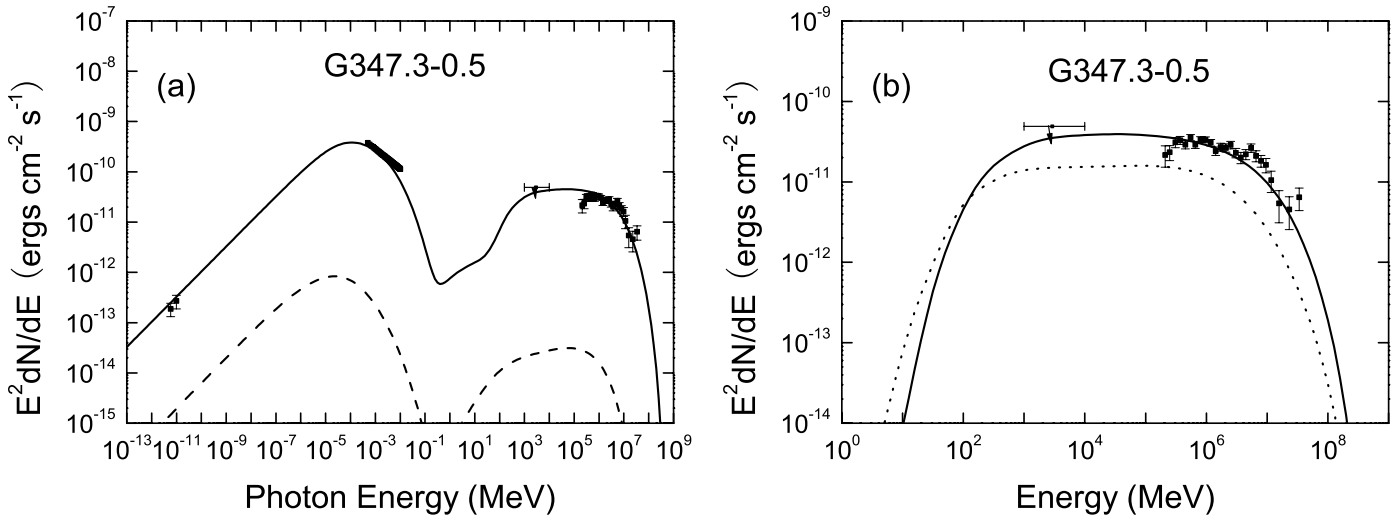

Fig. 1. a) Comparison of the model results with the multi-wavelength observations for the SNR G347.3−0.5. The emission from primary particles (electrons and protons), and secondary $e^{\pm}$ pairs are indicated by solid line and dashed line, respectively. **b)** The photon (solid line) and $\nu_\mu + \bar{\nu}_\mu$ (dotted line) spectra of the SNR produced from p-p interactions. The radio data (Lazendic et al. 2004), X-ray data (Slane et al. 1999), EGRET upper limit and VHE γ-ray data (Aharonian et al. 2006a) for the whole SNR are indicated. The parameters used are shown in Table 1.

synchrotron radiation of the primary electrons, whereas the observed TeV γ-rays are mainly from the p-p interactions between the accelerated protons and the ambient matter (see panel (a) in Fig. 1). Moreover, the γ-ray and $\nu_\mu+\bar{\nu}_\mu$ spectra resulting from the p-p interactions as high-energy protons collide with the ambient matter are shown in panel (b) in the figure. The number of $\nu_\mu+\bar{\nu}_\mu$ reaching the Earth is just about half of the original $\nu_\mu + \bar{\nu}_\mu$ number at the source due to flavor oscillations of neutrinos. Finally, the calculated neutrino event number for 5 yrs of observations with the 1 km^3 KM3NeT detector for energies above 1 TeV is about 8 (see Table 1), which is consistent with the result in Carr et al. (2007) because the resulting TeV γ-rays from the hadronic processes in our model dominate those from leptonic processes which is in agreement with the assumption in Carr et al. (2007).

3.2. G266.2−1.2

The HESS group reported its detection of TeV γ-rays from the shell-type SNR G266.2−1.2 (RX J0852.0-4622) on observations in February 2004 and the differential spectrum in the energy range from 500 GeV to 15 TeV is well described by a power law with a photon index of about 2.1 (Aharonian et al. 2005). Enomoto et al. (2006) reported the CANGAROO observations of the SNR, and the results are consistent with those detected with HESS. Furthermore, HESS re-observed the SNR between December 2004 and May 2005 for a total observation time of 33 h, above an average gamma-ray energy threshold of 250 GeV (Aharonian et al. 2007). The newest HESS observation results include more statistics especially at high energies and the spectrum extends from 300 GeV to 20 TeV with a spectral index of $2.24 \pm 0.04_{\rm stat} \pm 0.15_{\rm syst}$.

The SNR G266.2−1.2 was discovered by Aschenbach (1998) based on the X-ray data from the ROSAT All-sky survey. The SNR was observed with ASCA for 120ks and the X-ray spectra were featureless and well described by a power law (Slane et al. 2001). The X-ray spectral analysis of the whole remnant in the 2–10 keV energy band was also presented in Aharonian et al. (2007), and the non-thermal spectrum is well described by a power-law with a spectral index of 2.7 ± 0.2 and a flux of 13.8×10^{-11} erg cm^{-2} s^{-1} (Lemoine-Goumard et al. 2007). There are uncertainties in the distance and the age of the SNR. Bamba et al. (2005) derived an age of 425–1400 yr and a distance of 0.25–0.5 kpc based on observation of very thin hard X-ray filaments in the north-western edge with the high angular resolution of the Chandra satellite. In this paper, we use an age of 1000 yr and a distance of 0.3 kpc to model the non-thermal

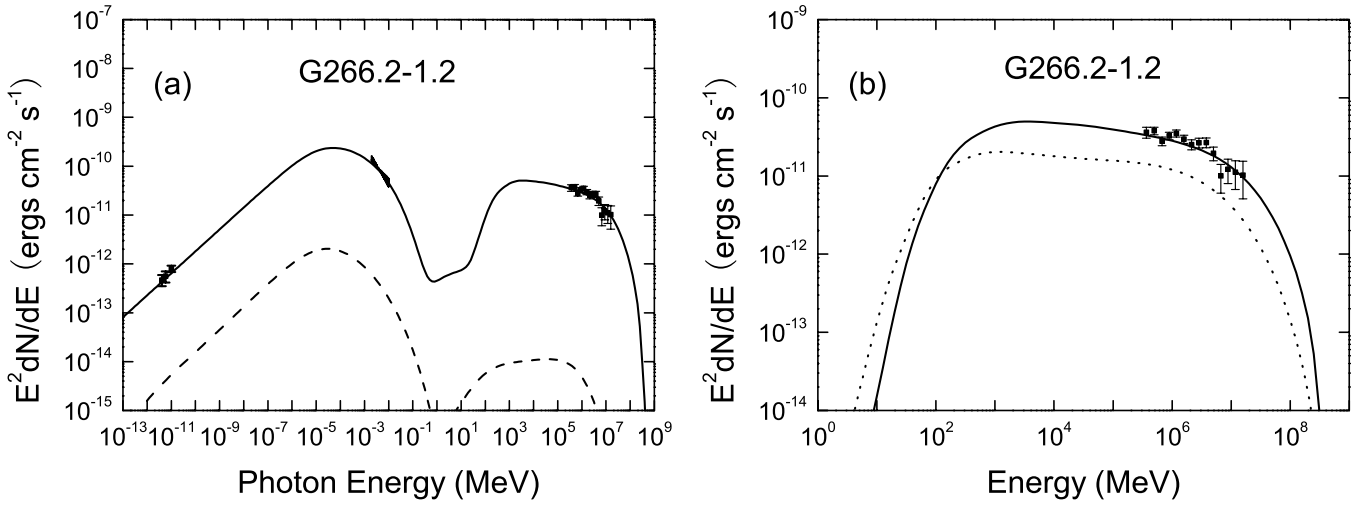

Fig. 2. a) Comparison of the model results with the multi-wavelength observations for the SNR G266.2−1.2. **b)** The photon (solid line) and $\nu_\mu + \bar{\nu}_\mu$ (dotted line) spectra of the SNR produced from p-p interactions. The radio data (Duncan and Green 2000), X-ray data (Lemoine-Goumard et al. 2007), and VHE γ-ray data (Aharonian et al. 2007), for the whole SNR are indicated. Others are the same as Fig. 1.

emission from the SNR. Details of the other parameters are shown in Table 1 and the resulting photon and neutrino spectra are illustrated in Fig. 2. The model results are consistent with the radio (Duncan and Green 2000), ASCA (Lemoine-Goumard et al. 2007) and HESS (Aharonian et al. 2007) observations; moreover, the VHE γ-rays from the SNR are produced mainly via p-p interactions. The expected event rates ($E_\nu > 1$ TeV) with KM3NeT after 5 yrs of observations is about 11, which makes it the source most likely be identified as a discrete neutrino source in the Galaxy by the next-generation km^3-scale neutrino telescopes.

3.3. G8.7−0.1

Aharonian et al. (2006b) reported a survey of the inner part of the Galactic Plane in VHE γ-rays detected with the HESS Cherekov telescope system. Fourteen previously unknown sources were detected. HESS J1804−216 is the brightest of the new sources, with a steep photon index of 2.72 ± 0.12 and a flux of nearly 25% of the flux from the Crab Nebula above 200 GeV. The source can be associated with the south-western part of the shell of the SNR G8.7−0.1 of radius 26 arc minutes with 80 Jy flux at 1 GHz (Aharonian et al. 2006b). Cui & Konopelko (2006) reported high-resolution X-ray observations taken with the Chandra X-Ray Observatory of the field that contains the TeV γ-ray source HESS J1804−216; a total of 11 discrete sources were detected. Among those sources, only one, CXOU J180351.4−213707, which is the most probable X-ray counterpart of HESS J1804−216, is significantly extended, with a photon index $1.2^{+0.5}_{-0.4}$.

In this paper, we assume that the sources CXOU J180351.4−213707 and HESS J1804−216 are associated with the SNR G8.7−0.1 at a distance of 6 kpc, and apply our model to it. To make the resulting spectrum consistent with the observations by Chandra with a low energy flux and a photon index of about 1.2, the SNR must be in the radiative phase when the roll-off energy of synchrotron radiation of the primary electrons decreases quickly and the X-rays detected by Chandra X-Ray Observatory are most probably from bremsstrahlung radiation or inverse Compton scattering of leptons (Fang & Zhang 2008). Thus, the highest-energy TeV photons are mainly from the p-p interactions as high-energy protons collide with the ambient matter in the SNR, and the proton hydrogen density $n_{\rm ISM}$ around the SNR must be about 6 cm^{-3} to make the calculation results consistent with the HESS observations. The details of the other parameters are given in Table 1. From Fig. 3, we have following results for the SNR: (i) the emission from the primary electrons dominates that from the secondary e$^\pm$ pairs in the entire energy band besides the narrow soft X-ray band around 0.5 keV; (ii) the detected radio emission is mainly from the synchrotron radiation of the primary electrons whereas the X-rays observed with Chandra are primarily produced via bremsstrahlung of these electrons; and (iii) the TeV photons with energies <1 TeV are primarily from both bremsstrahlung of the primary electrons and the p-p interaction of the primary protons. However, those with higher energies are mainly from the p-p interactions as the high-energy protons collide with the ambient matter.

In our model, for an SNR in the radiative stage, the sources of the primary particles are cut off and the primary electrons experience strong energy loss, whereas the secondary e$^\pm$ pairs can be produced continuously for a long time due to the large energy loss time for the p-p interaction. Therefore, the emission from the primary electrons diminishes quickly and that from the secondary e$^\pm$ pairs becomes more and more prominent as the SNR ages. Moreover, the high-energy protons also experience energy loss due to the p-p interactions and escape from the SNR. The secondary products from the p-p interactions are also deceasing as the age of the SNR increases. As a result, the expected event rates of the SNR G8.7−0.1 with KM3NeT in 5 yrs of observations is only about 0.9, which is about an order of magnitude smaller than that for the young SNRs G347.3−0.5 and G266.2−1.2.

3.4. G23.3−0.3

HESS J1834−087 is another extended TeV source recently discovered in the HESS survey of the inner Galaxy in VHE γ-rays. The source, which is spatially coincident with the SNR G23.3−0.3 (W41), has a size of 12 arc minutes and a γ-ray flux of 8% of the flux from the Crab Nebula above 200 GeV, with a photon index of 2.45 ± 0.16 (Aharonian et al. 2006b). Albert et al. (2006) presented the observations

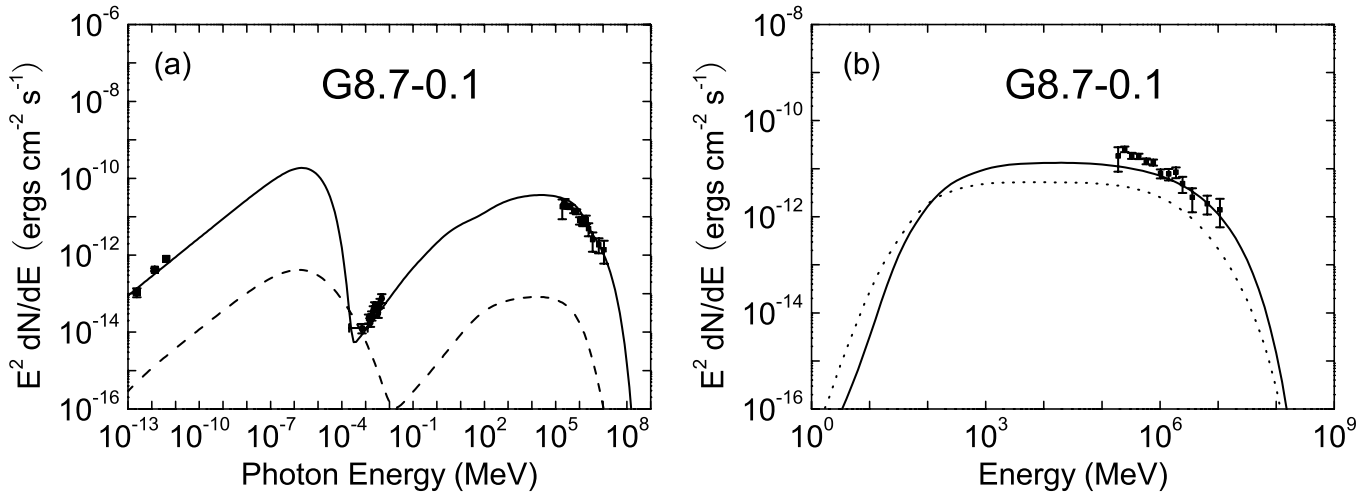

Fig. 3. a) Comparison of the model results with the multi-wavelength observations for the SNR G8.7−0.1. **b)** The photon (solid line) and $\nu_\mu + \bar{\nu}_\mu$ (dotted line) spectra of the SNR produced from p-p interactions. The radio data (Odegard et al. 1986; Kassim & Weiler 1990; Green 2006), X-ray data (Cui & Konopelko 2006), and VHE γ-ray data (Aharonian et al. 2006b; Enomoto et al. 2006) for the whole SNR are indicated. Others are the same as Fig. 1.

of HESS J1834−087 with the Major Atmospheric Gamma Imaging Cherenkov telescope (MAGIC), and the differential γ-ray flux can be expressed as $dN/dAdtdE = (3.7 \pm 0.6) \times 10^{-12}(E/\mathrm{TeV})^{-2.5\pm0.2}$ cm^{-2} s^{-1} TeV^{-1}.

G23.3−0.3 is an asymmetric shell-type SNR, and has a spectral index of 0.5 and a flux of 70 Jy at 1 GHz (Green 2006). Tian et al. (2007) reported new HI observations from the VLA Galactic Plane System and a new XMM-Newton observation for HESS J1834−087. They estimated that G23.3−0.3 is an old SNR with a distance of 4 ± 0.2 kpc and an age of ∼10^5 yr. The new XMM-Newton observation reveals diffuse X-ray emission within the HESS source and suggests an association between the X-ray and the VHE γ-ray emission. More recently, Leahy & Tian (2008) measured a distance of 3.9–4.5 kpc with high precision for the SNR with HI and CO line observations, which is direct evidence supporting that W41 is physically associated with the giant molecular cloud at a radial velocity of ∼78 km s^{-1} in the direction of the center of W41. Furthermore, the matter density around the SNR will be 2 to 3 times larger than previously estimated (6 cm^{-3}), but uncertainties also exist because there are a few adjustable parameter assumptions in estimating the density (Tian, W. W. private communication).

Finally, we use a distance of 4.2 kpc and an age of 80 000 yr to model the non-thermal spectrum for the SNR. The other parameters are shown in Table 1 and the resulting photon and neutrino spectra are illustrated in Fig. 4. The observed radio and VHE γ-ray emissions can be reproduced well by a synchrotron mechanism for the primary electrons and the p-p interactions of the high-energy protons; the emission from secondary $e^{\pm}$ pairs dominates that from the primary electrons in the energy band from about 0.1 eV to 0.5 keV. For the old SNR G23.3−0.3, the expected event rates at KM3NeT after 5 yrs of observations is about 0.5. Therefore, the SNR is more difficult to identify as a discrete neutrino source with neutrino telescopes than the other three sources, G347.3−0.5, G266.2−1.2, and G8.7−0.1.

4. Discussion and conclusions

VHE γ-rays from a few shell-type SNRs have been reported. The resulting TeV γ-rays can be produced either via inverse Compton scattering and/or via the p-p interaction. In the latter case, the TeV γ-rays are of hadronic origin, and then the number of neutrinos from SNRs should be significant, making SNRs are important possible neutrino sources in the Galaxy as a target for the next-generation km^3-scale neutrino telescope, KM3NeT. In this paper, based on a time-dependent model of non-thermal particle and photon spectra for both young and old SNRs, we investigate the possible neutrino emission from two young and two old SNRs and estimate the event rates expected for the four sources to be observed with KM3NeT using the newest simulation results given by Carr et al. (2007). Firstly, the unknown parameters can be limited by comparison of the model result with the multi-band photon observations for a given SNR; then the neutrinos from the SNR can be investigated. The calculation results show that the TeV γ-rays with energies above 1 TeV from the four sources primarily have a hadronic origin. The predicted neutrino spectra are shown in Figs. 1–4. The number of $\nu_\mu + \bar{\nu}_\mu$ signals reaching the Earth from an SNR is about half of the original number at the source due to flavor oscillations of neutrinos. The expected event rates at next-generation neutrino telescope KM3NeT after 5 yrs of observations of the four sources are shown in Table 1. Our results indicate that young SNRs such as G266.2−1.2 and G347.3−0.5 are the potential neutrino sources whose neutrinos are the most likely to be identified by the next-generation km^3 neutrino telescope. Our results justify the assumption proposed by many other authors that the high-energy TeV γ-rays from SNRs are produced mainly through hadronic interactions. However, due to the many uncertainties for a given SNR involved in the model such as the initial ejecta mass, the initial shock velocity, age, distance, and uncertainties in the multi-band observations, especially in the X-ray band, the results in Table 1 are rough approximations of the event rates potentially detected by KM3NeT.

We estimate the possible neutrinos observed from SNRs with KM3NeT using a time-dependent model by limiting the unknown parameters to improve consistency of the model result with the multi-band observations for each SNR. Of course, GLAST will provide a much more significant limitation on the parameters and check the correctness of our calculation more effectively due to its high sensitivity in the energy range from 30 MeV to 300 GeV. SNRs with detected VHE γ-rays are good candidates for high-energy neutrino observations with

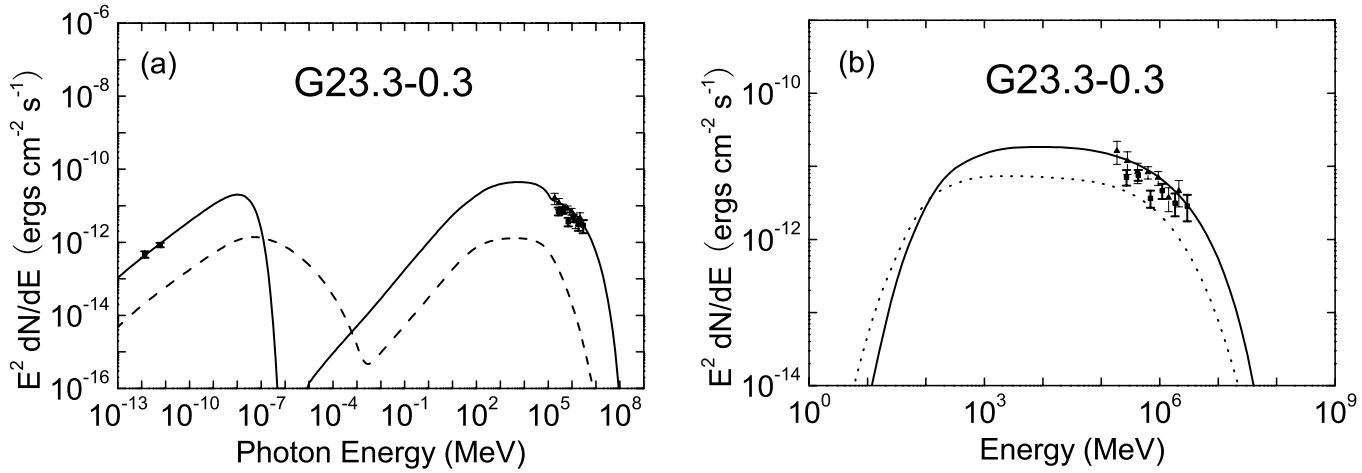

Fig. 4. a) Comparison of the model results with the multi-wavelength observations for the SNR G23.3−0.3. **b)** The photon (solid line) and $\nu_\mu + \bar{\nu}_\mu$ (dotted line) spectra of the SNR produced from p-p interactions. The radio data (Tian et al. 2007) and VHE γ-ray data (Aharonian et al. 2006b; Albert et al. 2006) for the whole SNR are indicated. Others are the same as Fig. 1.

next-generation km^3-scale neutrino telescopes. It is widely accepted that SNRs are the prime sites accelerating cosmic rays in the Galaxy, and the observations of neutrinos from SNRs will substantially improve our understanding of the acceleration mechanism and the hadronic processes involved in SNRs.

Acknowledgements. This work is partially supported by a Distinguished Young Scientists grant from the National Natural Science Foundation of China (NSFC 10425314), NSFC grant 10778702, and a grant from the Department of Education of Yunnan Province (07J51074). We appreciate the use of the high performance computer facilities at Yunnan University, Kunming, PRC.

References

Aharonian, F., Akhperjanian, A. G., Bazer-Bachi, A. R., et al. (HESS Collaboration) 2005, A&A, 437, L7
Aharonian, F., Akhperjanian, A. G., Bazer-Bachi, A. R., et al. (HESS Collaboration) 2006a, A&A, 449, 223
Aharonian, F., Akhperjanian, A. G., Bazer-Bachi, A. R., et al. (HESS Collaboration) 2006b, ApJ, 636, 777
Aharonian, F., Akhperjanian, A. G., Bazer-Bachi, A. R., et al. (HESS Collaboration) 2007, ApJ, 661, 236
Albert, J., Aliu, E., Anderhub, H., et al. (MAGIC Collaboration) 2006, ApJ, 643, L53
Aschenbach, B. 1998, Nature, 396, 141
Bamba, A., Yamazaki, R., & Hiraga, J. S. 2005, ApJ, 632, 294
Bednarek, W., Burgio, G. F., & Montaruli, T. 2005, NewAR, 49, 1
Carr, J., Dornic, D., Jouvenot, F., et al. 2007, [arXiv:0711.2145]
Cavasinni, V., Grasso, D., & Maccione, L. 2006, APh, 26, 41
Costantini, M. L., & Vissani, F. 2005, APh, 23, 477
Cui W., & Konopelko A. 2006, ApJ, 652, L109
Duncan, A. R., & Green, D. A. 2000, A&A, 364, 732
Ellison, D. C., Patnaude, D. J., Slane, P., et al. 2007, ApJ, 661, 879
Enomoto, R., Tanimori, T., Naito, T., et al. 2002, Nature, 416, 823
Enomoto, R., Watanabe, S., Tanimori, T., et al. 2006, ApJ, 652, 1268
Fang J., & Zhang L. 2008, MNRAS, 384, 1119
Hillas, A. M. 2005, J. Phys. G, 32, R95
Green D. A. 2006, A Catalogue of Galactic Supernova Remnants (2006 April version). Astrophysics Group, Cavendish Laboratory, Cambridge, UK
Kamae, T., Abe, T., & Koi, T. 2005, ApJ, 619, L163
Kamae, T., Karlsson, N., Mizuno, T., et al. 2006, ApJ, 647, 692
Kappes, A., Hinton, J., Stegmann, C., et al. 2007, ApJ, 656, 840
Kassim N. E., & Weiler, K. W. 1990, Nature, 343, 146
Katagiri, H., et al. 2005, ApJ, 313, 842
Kistler, M. D., & Beacom, J. F. 2006, Phys. Rev. D, 74, 063007
Lazendic, J. S., Slane, P. O., Gaensler, B. M., et al. 2004, ApJ, 602, 271
Leahy, D. A., & Tian, W. W. 2008, AJ, 135, 167
Lemoine-Goumard, M., et al. (HESS Collaboration) 2007, ICRC, [arXiv:0709.4621]
Odegard N. 1986, AJ, 92, 1372
Pannuti, T. G., Allen, G. E., Houck, J. C., et al. 2003, ApJ, 593, 377
Reynolds, S. P. 1996, ApJ, 459, L13
Slane, P., Gaensler, B. M., Dame, T. M., et al. 1999, ApJ, 525, 357
Slane, P., Hughes, J. P., Edgar, R. J., et al. 2001, ApJ, 548, 814
Sturner, S. J., Skibo, J. G., Dermer, C. D., et al. 1997, ApJ, 490, 619
Tian, W. W., Li, Z., Leahy, D. A., et al. 2007, ApJ, 657, L25
Vissani, F. 2006, Prepared for Vulcano Workshop 2006: Frontier Objects in Astrophysics and Particle Physics, Vulcano, Italy, 22–27 May 2006, [arXiv:astro-ph/0609575]
Wang, Z. R., Qu, Q. Y., & Chen, Y. 1997, A&A, 318, L59
Zhang, L., & Fang, J. 2007, ApJ, 666, 247